Tectonophysics 483 (2010) 214–222

Contents lists available at ScienceDirect

Tectonophysics

journal homepage: www.elsevier.com/locate/tecto

GPS-derived motion of the Adriatic microplate from Istria Peninsula and Po Plain sites, and geodynamic implications

John Weber [a,*], Marko Vrabec [b], Polona Pavlovčič-Prešeren [c], Tim Dixon [d], Yan Jiang [d], Bojan Stopar [c]

[a] Department of Geology, Grand Valley State University, 1 Campus Drive, Allendale, MI 49401 USA
[b] Department of Geology, University of Ljubljana, 12 Aškerčeva, 1000 Ljubljana, Slovenia
[c] Department of Geodesy, University of Ljubljana, 2 Jamova Cesta, 1000 Ljubljana, Slovenia
[d] Geodesy Lab, RSMAS-MGG, University of Miami, 4600 Rickenbacker Causeway, Miami, FL 33149 USA

ARTICLE INFO

Article history:
Received 25 September 2008
Received in revised form 1 September 2009
Accepted 2 September 2009
Available online 11 September 2009

Keywords:
Plate tectonics
Adriatic microplate
Alps
Apennines
GPS
Neotectonics

ABSTRACT

We studied the motion of the Adriatic microplate using Eurasian-referenced GPS-derived velocities from Istria Peninsula (Slovenia, Croatia) and Po Plain (Italy) sites and earthquake slip vectors around its edges from a Regional Centroid Moment Tensor catalogue. We explored kinematic parameters by inverting GPS velocities using a variety of site combinations and comparing results. Our best-fitting GPS Adria–Eurasia angular velocity vector (Euler pole) comes from 7 Istria Peninsula (Slovenia, Croatia) and 10 Po Plain (Italy) sites; it locates at 45.03°N, 6.52°E, with a 0.297 ± 0.116°/Myr counterclockwise rotation rate. This new GPS-derived pole locates and overlaps with our earthquake slip-vector-derived pole. An Adriatic microplate interpretation is at odds with Neogene geologic features that indicate recent convergence across the Apennines and Alps. The neotectonics–geology mismatch probably signals the recent birth of the Adria microplate upon termination of the Nubia–Eurasia Alpine collison and Adria slab break-off beneath the Apennines.

1. Introduction

The Mediterranean region is a complex tectonic patchwork of arcuate collisional mountain belts (Alps, Dinarides), old unsubducted Tethyian oceanic lithosphere (Ionian Sea), young oceanic rift basins (Tyhrrenian Sea), active (Calabrian Arc) and aborted subduction zones, accretionary prisms (Appenines), and microplates (Fig. 1). This level of complexity is surprising given the nearly head-on and long-lived Nubia–Eurasia collision that drives the system (Dewey et al., 1973; DeMets et al., 1990,1994). Much of it is related to unexpected "sideways" (plate-margin parallel and oblique) motions that reflect local tectonic escape, upper-plate effects from slab pull and hinge roll back, and microplate motion.

McKenzie (1972) first proposed the existence of an Adriatic microplate that moves independently of both Africa (Nubia) and Eurasia in the Mediterranean. Anderson and Jackson's (1987) analysis of earthquake slip-vectors determined for the large ($m_b > 5.5$) earthquakes that rimmed the deforming edges of the aseismic Adriatic core showed consistent NE–SW extension in the Apennines, N–S shortening in northern Italy, and NE–SW shortening in Croatia and Albania, suggesting the presence of a microplate rotating counterclockwise about a nearby pole. Despite this relatively coherent slip-vector pattern, the microplate model was not widely accepted, in part, because it is at odds with Neogene geologic features that indicate recent convergence across the Apennines and Alps (e.g., Platt et al., 1989; Selvaggi and Amato, 1992; Favali et al., 1993; Italiano et al., 2000; Wortel and Spakman, 2000).

Most of the stable aseismic interior of Adria is submerged beneath seawater, impinged on by young thrust faults, and, in the Po Plain, covered by a thick blanket of young unconsolidated alluvial sediment (Fig. 1). Even with the inherently limited distribution of available sites and potential for alluvial site instability, seminal space geodetic studies began to corroborate the existence of an Adriatic microplate, and, using more and better data, geodetic studies are now beginning to refine the Anderson and Jackson (1987) model (Ward, 1994; Calais et al., 2002; Battaglia et al., 2004; Grenerczy et al., 2005; Serpelloni et al., 2005; Devoti et al., 2008; D'Agostino et al., 2008). Slip-vectors from a recent and up-to-date Regional Centroid Moment earthquake catalogue (Pondrelli et al., 2006; http://www.bo.ingv.it/RCMT/Italydataset.html) also provide additional high-quality kinematic constraints (D'Agostino et al., 2008).

Ward (1994), using VLBI data, published the first space geodetic study of the Adria microplate. Calais et al. (2002) simultaneously inverted GPS velocities from only two continuous GPS sites in the Po

* Corresponding author.
E-mail addresses: weberj@gvsu.edu (J. Weber), vrabec.marko@gmail.com (M. Vrabec), ppavlovc@fgg.uni-lj.si (P. Pavlovčič-Prešeren), tdixon@rsmas.miami.edu (T. Dixon), yjiang@rsmas.miami.edu (Y. Jiang), bojan.stopar@fgg.uni-lj.si (B. Stopar).

0040-1951/$ – see front matter © 2009 Elsevier B.V. All rights reserved.
doi:10.1016/j.tecto.2009.09.001

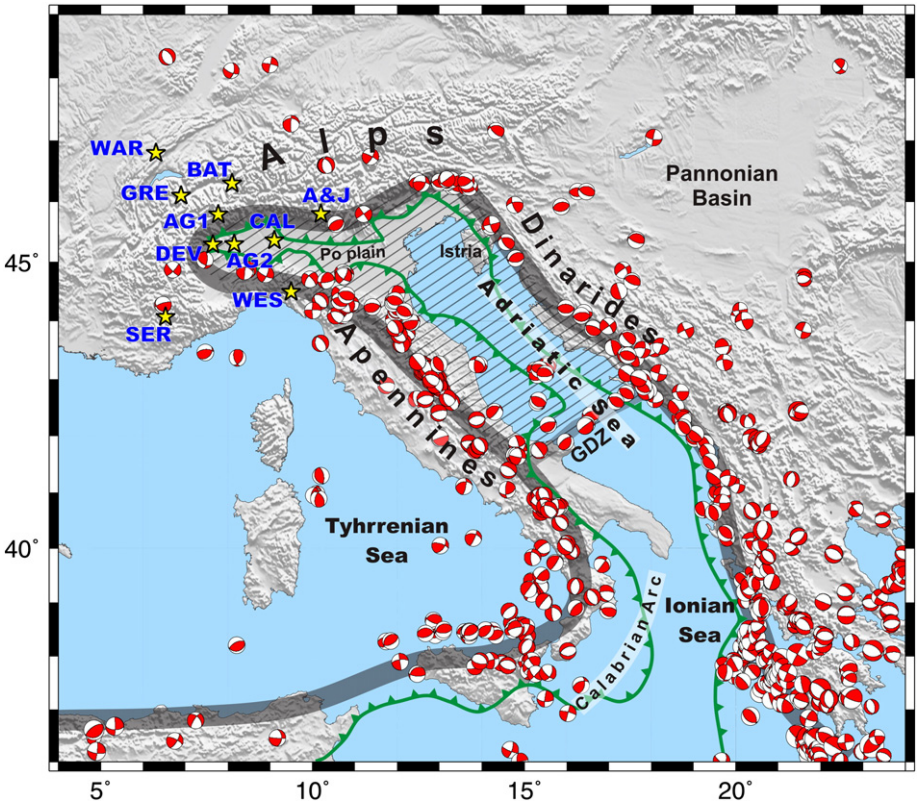

Fig. 1. Map showing circum-Adriatic topography, seismicity, and earthquake focal mechanisms taken from the 1976–2008 Italian CMT dataset (Pondrelli et al., 2006; http://www.bo.ingv.it/RCMT/Italydataset.html) and the 1997–2008 European-Mediterranean RCMT database (http://www.bo.ingv.it/RCMT/). The heavy grey lines separate the Adriatic microplate (largely aseismic; diagonally patterned) from possible additional microplates (not shown) and Nubian (African) lithosphere to the south, and Eurasian lithosphere to the north, east, and west. The Gargano–Dubrovnik zone (GDZ) is taken as the southern boundary of the Adriatic microplate. Green line shows deformed (thrust) margin front around Adriatic region (part active; part inactive) with sawteeth on upthrust side. Yellow stars depict published locations of Adria–Eurasia Euler poles: A&J—Anderson & Jackson (1987); WES—Westaway (1992); WAR—Ward (1994); CAL—Calais et al. (2002); BAT—Battaglia et al. (2004) Northern Adriatic; GRE—Grenerczy et al. (2005) Northern Adriatic; SER—Serpelloni et al. (2005); DEV—Devoti et al. (2008); AG1—D'Agostino et al. (2008) GPS-derived solution; AG2 D'Agostino et al. (2008) slip vector-derived solution.

Plain, UPAD and TORI, together with Anderson and Jackson's (1987) slip vector data set, deriving an Adria–Eurasia angular velocity vector similar in position to Anderson and Jackson's (1987) pole of rotation. Calais et al. used this constraint, together with the inferred curved western Adria–Eurasia boundary (Fig. 1), to explain the unexpected dextral shear and extension that they observed geodetically in the western Alps, where clearly collision and thrusting seem to have ceased. Battaglia et al. (2004) used ~50 circum-Mediterranean GPS sites to simultaneously study Adria motion and elastic strain along model edges, and to test whether Adria could be separated into two blocks north and south of the Gargano–Dubrovnik zone (Fig. 1); Grenerczy et al. (2005) and Serpelloni et al. (2005) performed similar wide-aperture GPS studies; and D'Agostino et al. (2008) and Devoti et al. (2008) presented recent robust kinematic analyses and developed models using data from a large number of GPS sites.

Battaglia et al.'s (2004) and D'Agostino et al.'s (2008) analyses suggested an Adria-southern microplate (Apulia) boundary in the central Adriatic along the Gargano–Dubrovnik seismic belt (Fig. 1). Oldow et al. (2002) however presented a very different and testable view of Adriatic kinematics. By combining GPS velocities from their Italian Peri-Tyrrhenian Geodetic Array (PTGA) and the EUREF network with those from the eastern Adriatic CRODYN network (Altiner, 2001), they reproposed that the Adriatic is an African (Nubian) promontory that is fragmenting along a complex boundary into a Eurasia-attached northwestern block and a Nubia-attached southeastern block. We follow Battaglia et al. (2004) and D'Agostino et al. (2008) here and treat only the northern segment of Adriatic lithosphere north of the Gargano–Dubrovnik zone. Using new, previously unavailable data from the Istria Peninsula (Croatia and Slovenia) we explored whether the microplate, now well defined in the Po Plain by the studies described above, extends eastward to Istria across Oldow et al.'s (2002) sub-block boundary.

If microplate or block boundaries are well defined, techniques that simultaneously estimate the angular velocity of the block or microplate and edge (boundary) effects associated with elastic strain accumulation may be preferred. However, if block boundaries are not well defined or are diffuse (as is likely in the northeastern Adriatic), it may be advisable to take a more conservative approach, using only

Table 1
Continuous GPS sites on the Po plain, Italy and data spans processed in this study.

Continuous site name	Latitude (°N)	Longitude (°E)	Height (m)	Data interval processed	Data span (yrs)	Network
BOLG	44.500	11.357	99.67	04Sept–08Nov	4.2	Unknown
CANV	46.008	12.435	965.92	04May–08Aug	4.2	FredNet
CAVA	45.479	12.583	47.77	01Jul–08Nov	7.3	Venezia
COMO	45.802	9.096	292.27	04May–08Nov	4.5	Unknown
IENG	45.015	7.639	316.62	04Jan–08Nov	4.9	Unknown
MDEA	45.924	13.436	165.70	03Jan–08Sept	5.6	FredNet
MEDI	44.520	11.647	50.02	96Mar–08Nov	12.2	Euref
PADO	45.411	11.896	64.69	01Nov–08Nov	7.0	IGS
TORI	45.063	7.661	310.75	97Apr–08Nov	10.7	Euref
TRIE	45.710	13.763	323.42	03Feb–08Aug	5.5	FredNet
UDI1	46.037	13.253	149.30	06Apr–08Aug	2.4	FredNet
UDIN	46.037	13.253	146.03	02Jun–06Sept	4.2	FredNet
UPAD	45.407	11.878	84.09	95Feb–01Nov	6.8	Euref
VENE	45.437	12.332	67.20	96Aug–07Jul	10.1	Euref
VOLT	45.385	11.911	53.41	01Jul–08Nov	7.3	Venezia

geodetic sites that are located in the stable interior to define the block or microplate angular velocity. We took a middle-ground approach in this study. We assessed kinematic parameters and estimated microplate motion by first deriving site velocities using publicly available data from a large number of continuous GPS sites in the Po Plain (Table 1), and new data from seven episodic Istria Peninsula GPS sites (Fig. 2). We next inverted various subsets of these data for angular velocity vectors, transformed the velocities into a stable Eurasian reference frame, and compared and assessed results using goodness of fit criteria and residuals. A major contribution of this study is that we present and use previously unavailable GPS data from seven episodic sites in the Istria Peninsula (Slovenia and Croatia), which is the largest land promontory not covered by alluvium that extends into the rigid interior of the microplate (Fig. 1). We derived velocities for these sites using high-quality and long-duration GPS data collected between 1994 and 2003–2004 (Fig. 2). The 2003–2004 data were collected as part of the more extensive PIVO-2003 Slovenia GPS campaign that is described in Weber et al. (2006). Finally, we tested our best-fitting GPS-derived Adria–Eurasia angular velocity vector with a pole derived using earthquake slip vectors from Pondrelli et al.'s (2006) Regional Centroid Moment Tensor catalogue.

2. GPS data and data analysis

We analyzed both continuous and campaign-style GPS data following the methods outlined in Dixon et al. (1997) and Sella et al. (2002). We used the GIPSY software and Jet Propulsion Laboratory (JPL) satellite ephemeris and clock files (Zumberge et al., 1997). We processed all data that we had available for continuous sites, which, in some cases extended back to 1996 (Tables 1 and 2). To increase the accuracy of velocity determinations, we inserted offsets where significant jumps were observed in continuous time series, and solved

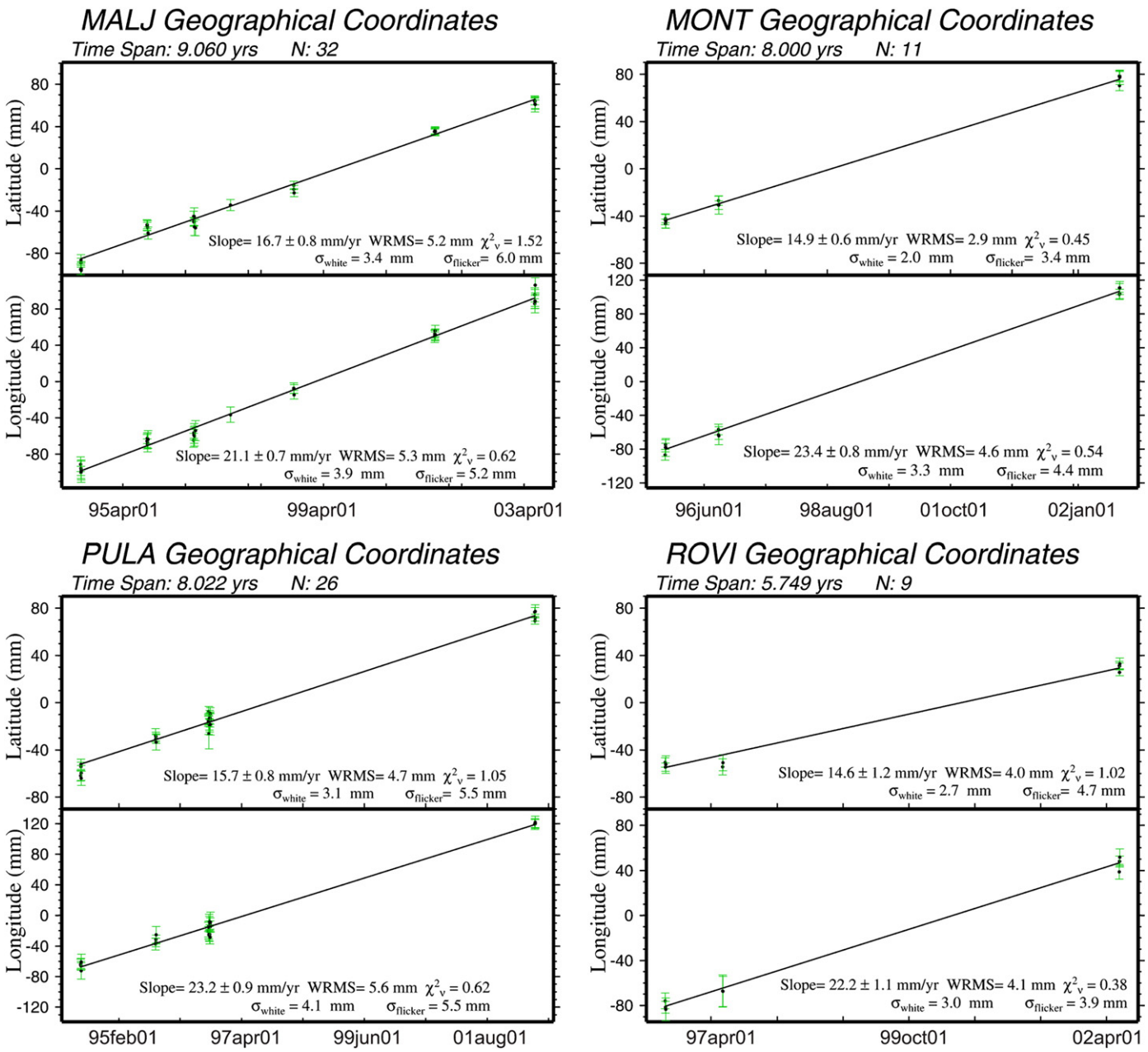

Fig. 2. GPS time series plots in the IGSB00 reference frame for the seven episodic Istria peninsula sites showing measurement history, data span and quality, and calculated components of horizontal velocity.

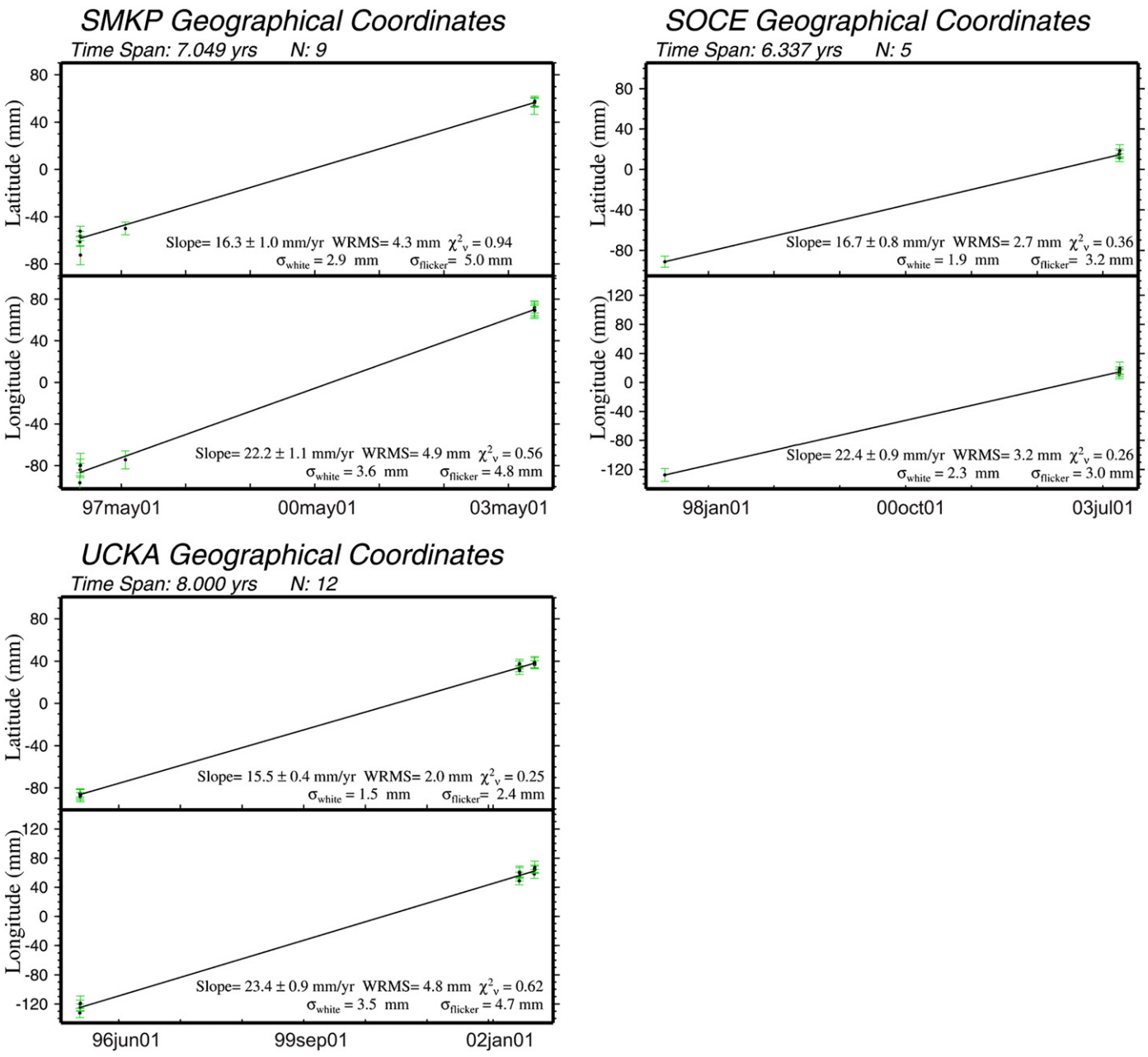

Fig. 2 (*continued*).

for site velocities around, rather than across, the jumps. We derived site velocities for the episodic Istria sites using the entire time series of data available for each site (Fig. 2). Data collection for these sites began in 1994, and repeat measurements were made in 1995, 1996, 1997, 1998, 2001, and 2003–2004. Data were collected in 3–15 day sessions. Many days involved 12–24 hour observation sessions.

We first derived site velocities in IGSB00, which is approximately equivalent to the global ITRF-2000 reference frame (International Terrestrial Reference Frame 2000) (Boucher et al., 2004). Site velocity uncertainties were estimated following Mao et al. (1999) and Dixon et al. (2000).

We next followed Sella et al. (2002) in defining a Eurasian reference frame, and used 15 continuous GPS sites on the stable Eurasian shield and platform south of the northern zone of rapid post-glacial rebound, and north of the southern Alpine–Himalaya deforming zone. Table 2 lists the 15 Eurasian reference sites, gives approximate locations, and lists the data spans that we processed for each.

Table 2
GPS sites and data spans processed to define stable Eurasian plate reference frame.

Site name	Latitude (°N)	Longitude (°E)	Height (m)	Data interval processed	Data span (yrs)	Network
ARTU	56.430	58.560	247.57	99Aug–03Jul	3.9	NEDA
BOGO	52.476	21.035	149.62	97Jan–03Jun	6.5	EUREF
BOR1	52.280	17.073	124.37	94Sep–03Jun	8.7	EUREF
GLSV	50.364	30.497	226.33	98Feb–03Jun	5.3	EUREF
GOPE	49.914	14.786	592.59	95Sep–03May	7.6	EUREF
JOZE	52.097	21.032	141.50	93Aug–03Jun	9.8	EUREF
KSTU	55.993	92.794	210.02	97Aug–03Jun	5.8	IGS
LAMA	53.892	20.670	187.02	94Dec–03Jun	8.5	EUREF
MDVO	56.027	37.224	254.86	95Feb–03Jan	7.9	EUREF
NYAL	78.930	11.865	78.52	93Jan–03Jun	9.2	EUREF
POTS	52.379	13.066	144.42	94Oct–03Jun	8.7	EUREF
TIXI	71.634	128.866	47.06	98Oct–03Jun	4.7	NEDA
WROC	51.113	17.062	180.81	97Apr–03May	6.1	EUREF
WTZR	49.144	12.879	666.04	96Jan–03Jun	7.4	EUREF
ZWEN	55.699	36.759	205.01	95Apr–03Mar	7.9	EUREF

Table 3
Istria and Po plain GPS site velocities and uncertainties in IGSB00 and Eurasian reference frames.

			IGSB00		Stable Eurasia	
Site ID	Latitude (°N)	Longitude (°E)	V_n (mm/yr)	V_e (mm/yr)	V_n (mm/yr)	V_e (mm/yr)
BOLG	44.50	11.36	17.50 ± 0.40	19.60 ± 0.70	3.79 ± 0.42	−1.40 ± 0.73
CANV	46.01	12.44	15.60 ± 0.60	20.70 ± 0.40	2.00 ± 0.62	−0.16 ± 0.44
CAVA	45.48	12.58	16.60 ± 0.20	20.80 ± 0.20	3.01 ± 0.24	−0.20 ± 0.28
COMO	45.80	9.10	12.70 ± 0.40	19.90 ± 0.40	−1.23 ± 0.43	−0.43 ± 0.45
IENG	45.02	7.64	14.10 ± 0.40	19.80 ± 0.30	0.04 ± 0.43	−0.46 ± 0.36
MALJ	45.50	13.64	16.70 ± 0.80	21.10 ± 0.70	3.23 ± 0.81	−0.07 ± 0.73
MONT	45.25	13.73	14.90 ± 0.60	23.40 ± 0.80	1.44 ± 0.82	2.16 ± 0.61
MDEA	45.92	13.44	16.60 ± 0.30	20.40 ± 0.20	3.11 ± 0.33	−0.64 ± 0.28
MEDI	44.52	11.65	16.30 ± 0.20	23.00 ± 0.20	2.62 ± 0.24	1.95 ± 0.29
PADO	45.41	11.90	15.20 ± 0.30	21.10 ± 0.20	1.54 ± 0.33	0.21 ± 0.28
PULA	44.87	13.85	15.70 ± 0.80	23.20 ± 0.80	2.25 ± 0.92	1.86 ± 0.81
ROVI	45.08	13.63	14.60 ± 1.20	22.20 ± 1.10	1.13 ± 1.21	0.94 ± 1.21
SMKP	45.55	13.72	16.30 ± 1.00	22.20 ± 1.10	2.84 ± 1.12	1.03 ± 1.01
SOCE	45.59	13.87	16.70 ± 0.80	22.40 ± 0.90	3.25 ± 0.92	1.21 ± 0.81
TORI	45.06	7.66	14.80 ± 0.20	20.30 ± 0.20	0.74 ± 0.25	0.05 ± 0.28
TRIE	45.71	13.76	16.60 ± 0.30	20.60 ± 0.30	3.14 ± 0.33	−0.54 ± 0.36
UCKA	45.28	14.20	15.50 ± 0.40	23.40 ± 0.90	2.09 ± 0.92	2.09 ± 0.42
UDI1	46.04	13.25	15.90 ± 0.70	21.50 ± 0.60	2.39 ± 0.71	0.51 ± 0.63
UDIN	46.04	13.25	16.80 ± 0.50	20.30 ± 0.50	3.29 ± 0.52	−0.69 ± 0.54
UPAD	45.41	11.88	16.00 ± 0.40	21.90 ± 0.30	2.34 ± 0.42	1.01 ± 0.36
VENE	45.44	12.33	16.20 ± 0.30	21.70 ± 0.30	2.59 ± 0.33	0.74 ± 0.36
VOLT	45.38	11.91	16.00 ± 0.20	20.60 ± 0.20	2.34 ± 0.24	−0.30 ± 0.28

3. Angular velocity vector inversions

We derived angular-velocity vectors describing the motion of the Eurasian Plate and the (northern) Adria microplate relative to IGSB00 using the formal inversion procedures outlined in Ward (1990) and Mao (1998). In an attempt to identify and isolate possible edge effects, e.g. elastic strain accumulation on locked active plate-boundary faults (many of which are still under investigation in the northeastern Adriatic), we inverted separate sets of GPS velocity data from: the seven Istria sites, ten presumed microplate interior sites in western Istria and the central Po Plain, seventeen Istria and Po Plain sites that exclude far western and far southern Po Plain sites near the microplate edges, and all twenty-two sites (Table 4). We used χ^2 tests, assessed rate residuals, and used geologic reasoning to decide which site combination provided the best-fitting Adria angular velocity and to explore the position and nature of the microplate boundaries. Our best-fitting and test solution strategies are listed in Table 4.

4. Earthquake slip vectors

Earthquake slip vectors from plate boundaries provide information on relative plate motion across the boundaries. Inverting slip vectors can give a pole location and rotation sense, but no rotation rate. Such data provide an important independent test of GPS-derived Euler pole positions (e.g., D'Agostino et al., 2008). Following Battaglia et al. (2004) and D'Agostino et al. (2008), we drew the southern boundary of the Adria microplate at the Gargano–Dubrovnik zone (Fig. 1). Using the formal inversion techniques discussed above, we inverted

Table 4
Summary of published Adria–Eurasia angular velocity vectors and those determined in this study.

Solution	Latitude (°N)	Longitude (°E)	Rotation rate (°/Myr)	Error ellipse max (°)	Error ellipse min (°)	Az (°)	Rotation rate sigma	χ^2_ν	Mean rate residual (mm/yr)
Anderson and Jackson	45.80	10.20	N.D.	N.D.	N.D.	N.D.	N.D.	N.D.	N.D.
Westaway	44.5	9.5	N.D.	N.D.	N.D.	N.D.	N.D.	N.D.	N.D.
Ward	46.8 ± 2.5	6.3 ± 3.8	0.29	N.D.	N.D.	N.D.	0.06	N.D.	N.D.
Calais et al.	45.36	9.10	0.520	N.D.	N.D.	N.D.	N.D.	N.D.	N.D.
Battaglia et al. (NAd)†	46.3 ± 0.4	8.1 ± 0.7	0.90	N.D.	N.D.	N.D.	0.20	N.D.	N.D.
Grenerczy et al. (NAd)†	46.1	6.9	0.35	1.1	0.5	−77.6	0.07	3.14	N.D.
Serpelloni et al.	44.07	6.53	0.244	N.D.	N.D.	N.D.	0.017	N.D.	N.D.
Devoti et al.	45.29	7.65	0.216	1.0	0.4	90	0.022	1.72	0.023
D'Agostino et al.	45.79	7.78	0.309	0.3	0.2	−81.0	0.021	1.2	0.35
This study 7-site GPS§	46.51	10.22	0.450	3.64	0.44	−63.1	0.556	1.1	1.0
This study 10-site GPS#	45.06	4.63	0.217	6.13	0.62	85.4	0.236	2.7	1.0
This study 17-site GPS*	45.03	6.52	0.297	1.74	0.40	82.2	0.116	2.3	1.0
This study 22-site GPS††	45.20	6.99	0.341	0.62	0.37	82.8	0.056	4.8	1.1
This study slip-vector solution	45.59	6.29	N.D.	3.51	0.88	95.1	N.D.	N.D.	N.D.

Note: also see Fig. 1, 6.
N.D. = not determined.
†NAd = Northern Adriatic.
§Istria Peninsula sites-only (MALJ, MONT, PULA, ROVI, SMKP, SOCE, UCKA) solution.
#Western Istria Peninsula (MALJ, MONT, PULA, ROVI, SMKP) plus central Po Plain (CAVA, PADO, UPAD, VENE, VOLT) microplate interior site solution.
*Statistically best-fit solution (CANV, CAVA, MALJ, MDEA, MONT, PADO, PULA, ROVI, SMKP, SOCE, TRIE, UCKA, UDI1, UDIN, UPAD, VENE, VOLT) = all (see †† below) minus (BOLG, COMO, IENG, MEDI, TORI).
††All Istria Peninsula plus Po Plain sites solution (BOLG, CANV, CAVA, COMO, IENG, MALJ, MDEA, MEDI, MONT, PADO, PULA, ROVI, SMKP, SOCE, TORI, TRIE, UCKA, UDI1, UDIN, UPAD, VENE, VOLT).
All uncertainties (except this study, slip-vector solution given at 1*D*, 2σ level) given at 1*D*, 1σ, but are plotted on Figures at 1*D*, 2σ level.

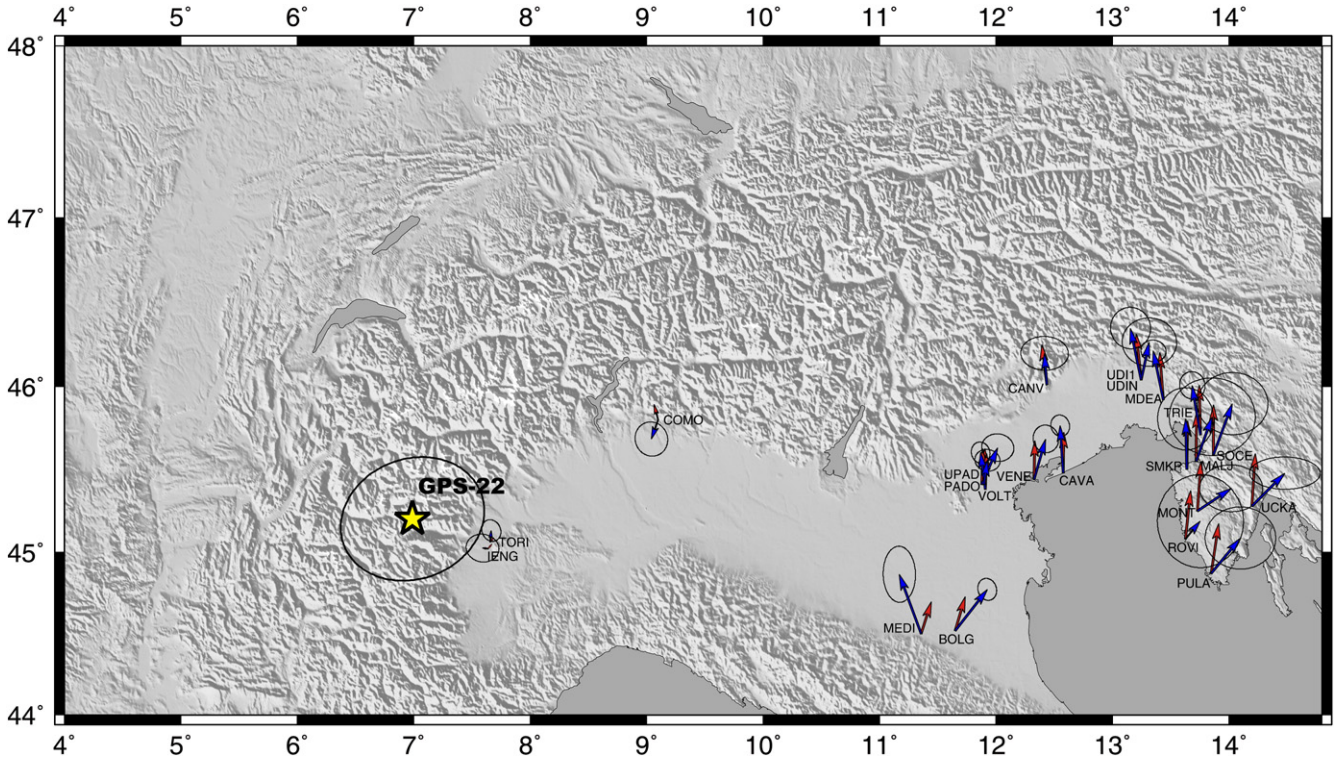

Fig. 3. GPS-derived twenty-two-site solution with Euler pole plotted at 1D, 2σ uncertainty, observed site velocities (blue arrows) with 1σ uncertainties, and predicted model site velocities (red arrows). Site velocities are shown in the Eurasian reference frame discussed in text.

earthquake slip vectors from Pondrelli et al.'s (2006; http://www.bo.ingv.it/RCMT/Italydataset.html) Regional Centroid Moment Tensor catalogue for events north of the Gargano–Dubrovnik zone and along the other inferred microplate boundaries. We derived an earthquake slip-vector pole to compare with our GPS-derived pole positions. The raw slip-vector data and solution are shown together on Fig. 5.

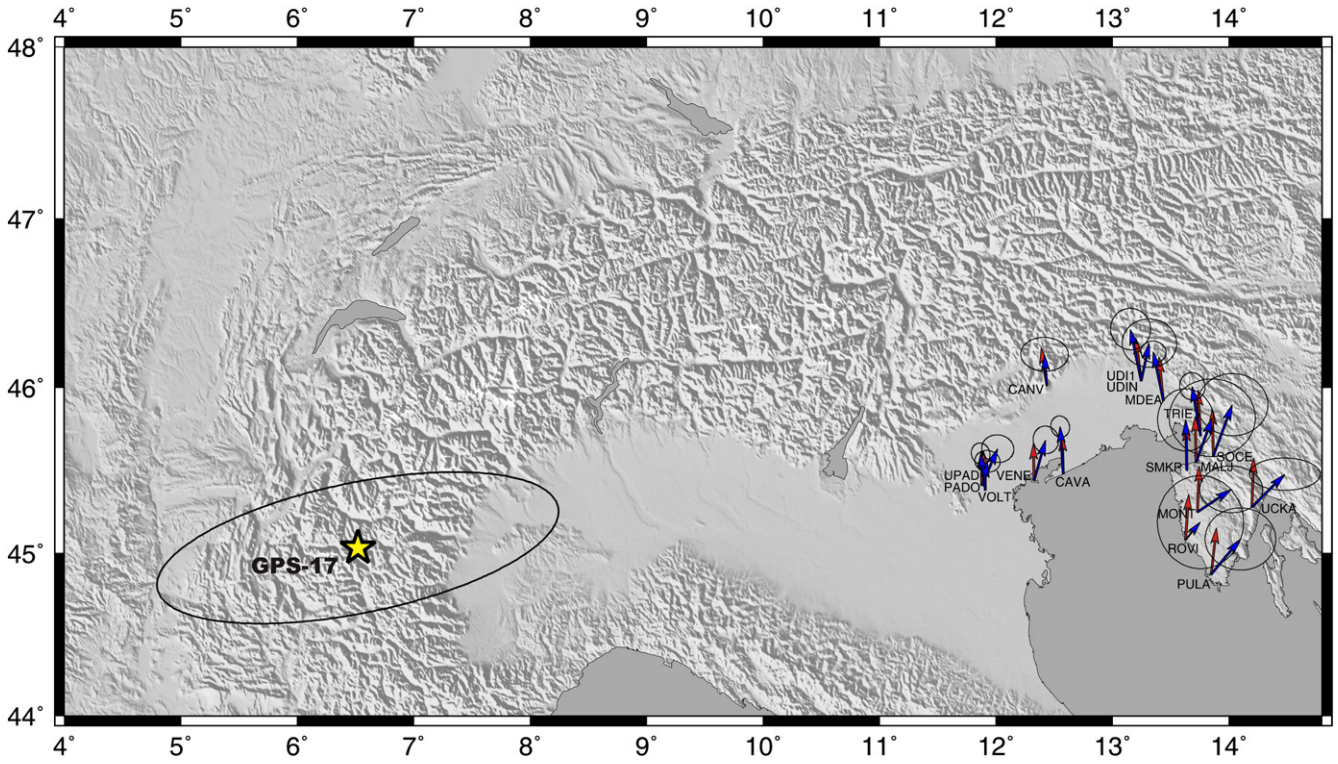

Fig. 4. GPS-derived seventeen-site solution with Euler pole plotted at 1D, 2σ uncertainty, observed site velocities (blue arrows) with 1σ uncertainties, and predicted model site velocities (red arrows). Site velocities are shown in the Eurasian reference frame discussed in text.

5. Results

5.1. Eurasian reference frame and GPS site velocities

The Eurasia-IGSB00 angular velocity reference vector we derived is located at 57.86°N, −101.56°E, with a 0.252 ± 0.003°/Myr rotation rate; the long axis of the $1-\sigma$ error ellipse is oriented toward 34.2° with a length of 1.14° and a short axis length of 0.28°. Site velocities determined in both the Eurasian and IGSB00 reference frames are given in Table 3. Sites on the Istria Peninsula move slowly relative to Eurasia, only a few mm/yr, but the motions are statistically significant and systematically oriented toward the NNE. The Eurasian-referenced site velocities for Po Plain sites are also slow and statistically significant, orient consistently toward the N, and systematically decrease in magnitude westward (Figs. 3 and 4). The systematic and consistent motions observed for the ensemble of Po Plain sites near Venice (CAVA, PADO, UPAD, VENE, VOLT) gave confidence that these are tectonic motions, not simply motions related to local lagoonal sinking (Figs. 3 and 4).

5.2. Adria–Eurasia angular velocity vectors

Results from the GPS velocity and earthquake slip-vector inversions are summarized in Table 4, shown in Figs. 3, 4, 5 and 6, and discussed below. Table 4 also gives a complete list of the sites used in each GPS solution.

Inversion of GPS velocities from the seven Istria peninsula sites yielded a well defined angular velocity vector, closest in position to the pole of Anderson and Jackson (1987) (Fig. 6), with a low mean rate residual, a low χ^2 (1.1), and no apparent systematic misfits. Residuals for sites MALJ and SOCE were slightly higher than the mean. This solution (46.51°N, 10.22°E, 0.450 ± 0.556) had high uncertainties in position and rate due to the small number of sites used and their limited geographic distribution.

In a ten-site solution, we inverted velocities from an ensemble of presumed microplate interior sites that were most distant from microplate boundaries, which could be accumulating elastic strain. Ten western Istria (MALJ, MONT, PULA, ROVI, SMKP) and central Po Plain (CAVA, PADO, UPAD, VENE, VOLT) sites were chosen. Rate residuals considerably above the mean, and systematic misfits, indicated that the velocities observed for MONT and ROVI, two of the five western Istria sites used, were misfit by this model; the χ^2 value obtained was 2.7, and this pole position (45.06°N, 4.63°E, 0.217 ± 0.236) shifted several hundred km from that for the seven-site solution discussed above (e.g., Fig. 6). Like the seven-site-solution, this solution had high uncertainties in position and rate due to the small number of sites used and their limited geographic distribution.

In our next solution, we used data from all twenty-two Po Plain and Istria sites. This solution provided the broadest geographic coverage available, but could have been affected by elastic or coseismic strain effects along the microplate edges. This solution has a high χ^2 (4.8) and edge sites BOLG, COMO, MONT, ROVI, and UCKA do indeed have rate residuals that exceed the mean (Fig. 3). In addition, the observed velocities at the southernmost Istria sites PULA, ROVI, UCKA, and MONT are systematically misfit by the model, and orient east of the predicted velocities, but generally fall within the observed uncertainties. Nonetheless, to demonstrate that adding data from the seven Istria sites improved estimation of the pole, we also ran a solution using data from only the fifteen Po Plain sites; this solution resulted in a higher χ^2 value of 5.7.

Our best-fitting, seventeen-site result (45.03°N, 6.52°E, 0.297 ± 0.116°/Myr counterclockwise rotation rate) was obtained using an

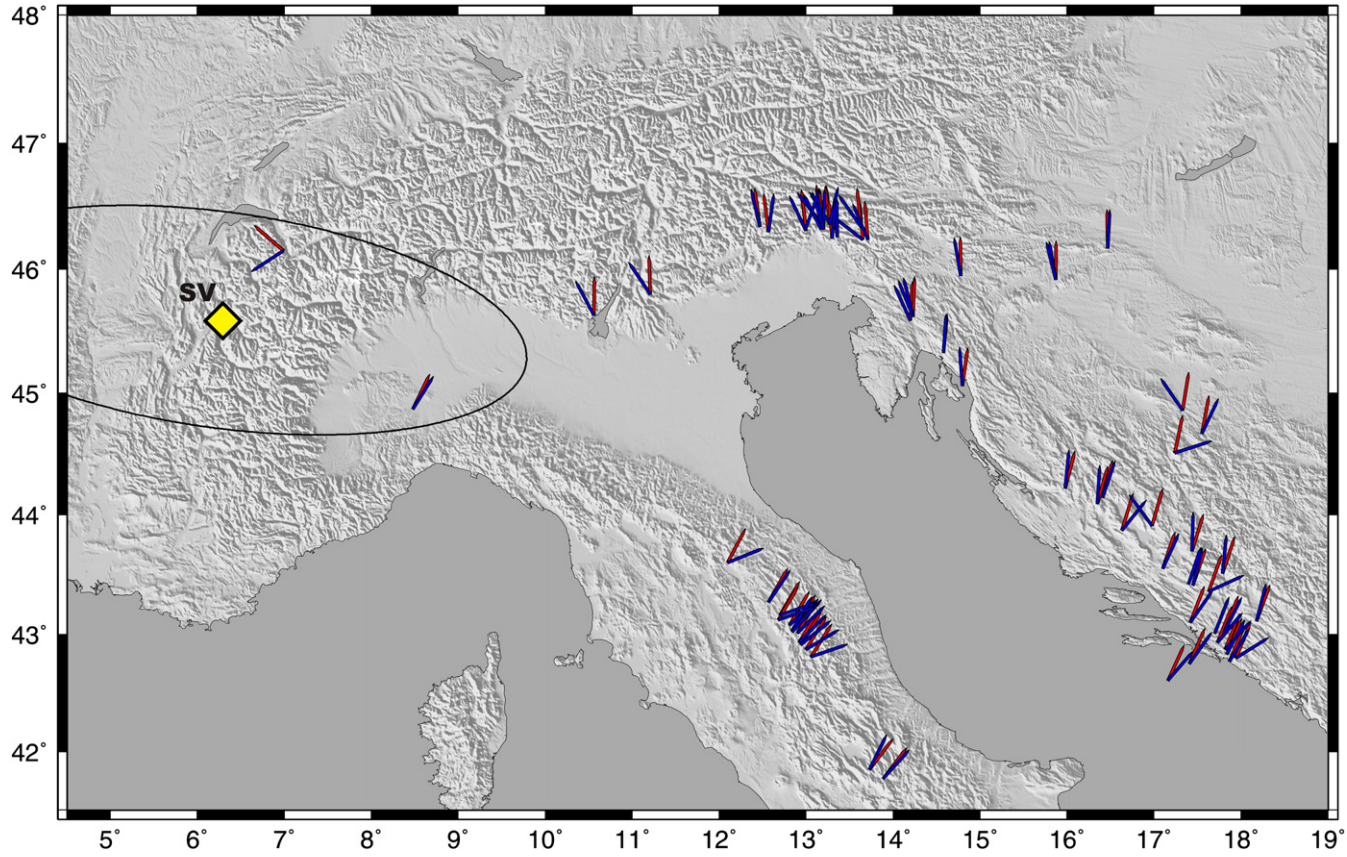

Fig. 5. Earthquake slip-vector-solution with Euler pole plotted at 1D, 2σ uncertainty, observed slip vectors (blue arrows), and predicted model slip vectors (red arrows). Slip vectors are taken from the 1976–2008 Italian CMT dataset (Pondrelli et al., 2006; http://www.bo.ingv.it/RCMT/Italydataset.html).

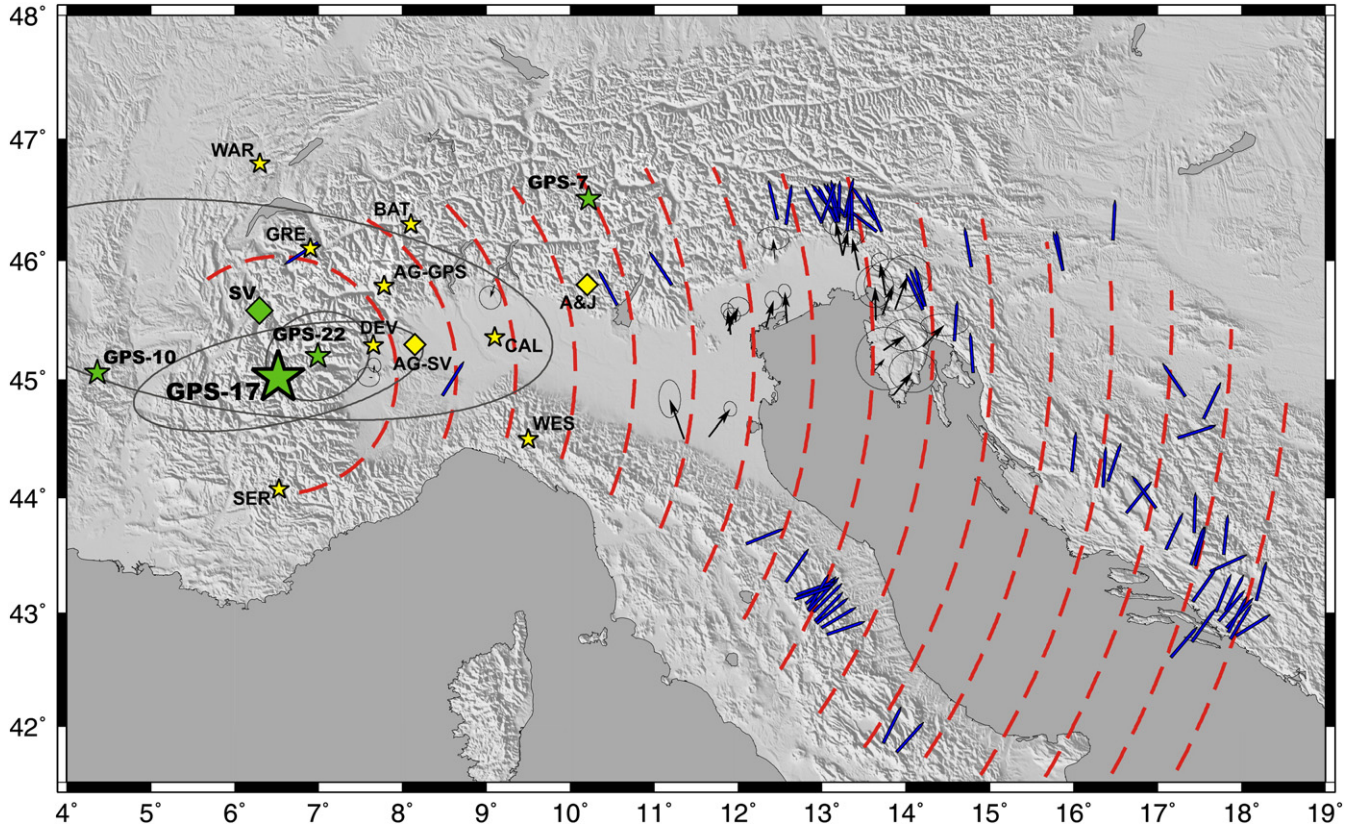

Fig. 6. Summary diagram showing observed GPS site velocities used in this study (with 1σ uncertainties), Adria–Eurasia Euler poles (diamonds: slip-vector-derived; stars: predominantly GPS-derived) determined in this study (green: GPS-7, GPS-10, GPS-17, GPS-22, and SV correspond to 7-, 10-, 17-, and 22-site GPS solutions and slip-vector-solution) and previously published (yellow): A&J—Anderson & Jackson (1987); WES—Westaway (1992); WAR—Ward (1994); CAL—Calais et al. (2002); BAT—Battaglia et al. (2004); GRE—Grenerczy et al. (2005); SER—Serpelloni et al. (2005); DEV—Devoti et al. (2008); AG-GPS—D'Agostino et al. (2008) GPS-derived solution; AG-SV D'Agostino et al. (2008) slip-vector-derived solution.

ensemble of the seven Istria sites together with ten Po Plain sites that exclude Po Plain sites (BOLG, COMO, IENG, MEDI, TORI) along the far western, southern, and northern edges of the microplate (Fig. 4). This result yielded a mean rate residual of 1.0 mm/yr, close to the velocity uncertainty, and a χ^2 of 2.3. Four of the Istria sites (MONT, ROVI, PULA, and UCKA) had rate residuals that were slightly above the mean and the same systematic direction misfits described above, again indicating either elastic strain accumulation along the eastern boundary of the microplate, inadequate determination of site velocities, or both (Fig. 4). The large observed velocity uncertainties for these three sites currently precludes a better interpretation.

Our earthquake slip-vector pole (45.59°N, 6.29°E E; counterclockwise rotation senses), is given in Table 4 and shown in Figs. 5 and 6, and within uncertainty, overlaps with our best-fitting GPS-derived Euler pole.

6. Discussion and conclusions

The Pondrelli et al. (2006) catalogue lists a series of M 4 thrust earthquakes that occurred during a two-week period in 2000, and a M 5.3 thrust that occurred in 2003, which locate within 50 km of the BOLG and MEDI sites. These events coincide in time with the span of GPS data that we processed for MEDI, but occurred before that which we processed for BOLG (Table 1). No obvious offsets were treated in the continuous time series for either site, but that for MEDI could contain subtle coseismic offsets. These observations suggest that elastic (interseismic) strain related to on-going thrusting affects the velocity at BOLG (Fig. 3). Similarly, the velocity at COMO is also likely affected by elastic strain accumulation related to on-going thrusting along the northern edge of the microplate. The high residuals and systematic misfits for the three eastern Istria sites in the seventeen-site-solution (Fig. 4) could be due to elastic strain accumulation along the eastern edge of the microplate, imprecise determination of site velocities using episodic data, or some combination. Acquiring additional GPS data at these sites, or adding data from continuous GPS sites in Istria should help to shrink velocity uncertainties and better resolve this issue.

That the new Eurasian-referenced Istria and Po Plain GPS motions change smoothly and uniformly across the region, and are well fit by a microplate model, strongly support that the entire region north of Gargano–Dubrovnik moves as a single block or microplate and is not cut by a major block-bounding fault (Fig. 1). A lack of data quantity and limited geographic spread caused inversions involving small subsets of data (our seven- and ten-site solutions) to give Euler pole positions that shifted by hundreds of km (Fig. 6). Better-defined Adria–Eurasia angular velocity vectors with overlapping pole positions and rates were obtained using more data, with a broader geographic spread (i.e. the seventeen- and twenty-two-site solutions) (Figs. 3, 4 and 6). Earthquake slip-vector inversions using high-quality data also gave an overlapping pole position (Fig. 5). Mean rate residuals for these seventeen- and twenty-two-site solutions suggest that the microplate may be rigid to within about 1 mm/yr (Table 4).

Previously published Adria–Eurasia pole positions together with our new estimates are summarized in Table 4 and plotted in Fig. 6. With the exception of those from a few of the earliest studies, we observe that pole position estimates have moved generally westward as the GPS and earthquake slip-vector data have increased in quality and quantity. Nonetheless, it is difficult to assess which of the poles in this cluster to choose as the best estimate.

Some logical steps for continuing to narrow this search would be: 1) to add more data for the episodic sites on the Istria Peninsula, and to add data from continuous GPS sites in Istria, 2) to add more data in

general from GPS sites in the eastern Adriatic, and 3) to add more GPS velocities from sites outside of the Po Plain-Istria region treated here, determine and compile spatially and geometrically accurate microplate boundaries, and simultaneously invert for Adria–Eurasia Euler poles and elastic plate-edge effects (see e.g. Battaglia et al., 2004).

The ~3 Ma timeframe NUVEL-1A geologic plate motion model predicts 9 mm/yr of 348°-directed relative Nubia–Eurasia plate motion near the Adriatic today (DeMets et al., 1990, 1994). The magnitude and direction of this predicted motion is distinctly different from the smoothly varying motions we observe across our Istria and Po Plain sites where a single microplate model fits the observed motions very well. This, plus the neotectonics—Neogene geology mismatch introduced above, implies that we are witnessing the end of the Nubia–Eurasia Alpine collision and the end of sub-Apennine subduction and the birth of a new microplate. The normal faults along the crest of the Apennines in Italy thus likely bound the western edge of the Adria microplate and do not reflect crustal extension in the upper-plate of an active Apennine-Adria subduction system. Sub-Apennine slab break-off within the past few Myr, together with a pinning of buoyant Adria lithosphere in the northern Po Plain, seems like a reasonable way to start Adria moving as an independent microplate (Malinverno and Ryan, 1986; Hippolyte et al., 1994; Wortel and Spakman, 2000; Stein and Sella, 2006). That the motion of Adria, not Nubia, drives active deformation in the northern Adriatic, has important implications for seismic risk assessment in the region—motion across Adria's boundary zones increase in a predictable way with distance from its pole of rotation. Our new GPS-based best-fitting angular velocity vector predicts extension in the central Appenines at rates of up to about 4 mm/yr, convergence in the Dinarides at $\leq$5 mm/yr, and is consistent with the right-lateral extrusion inferred along the northeastern (Slovenia) corner of the microplate (Fodor et al., 1998).

Acknowledgements

This work was supported by grants from the American Chemical Society—Petroleum Research Fund (40225-B8) and Slovene Ministry of Science. Zeljko Bačič and Florjan Vodopivec helped us obtain some of the Istria episodic GPS data and Pete La Femina helped with GPS data processing logistics. We also thank colleagues who run and maintain the various regional and global networks and publicly share the continuous GPS data used in this study.

References

Altiner, Y., 2001. The contribution of GPS to the detection of the Earth's crust deformations illustrated by GPS campaigns in the Adria region. Geophys. J. Int. 145, 550–559.

Anderson, H., Jackson, J., 1987. Active tectonics of the Adriatic region. Geophys. J. R. Astron. Soc. 91, 937–983.

Battaglia, M., Murray, M., Serpelloni, E., Burgmann, R., 2004. The Adriatic region: an independent microplate within the Africa–Eurasia collision zone. Geophys. Res. Lett. 31, L09605. doi:10.1029/2004GL019723.

Boucher, C., Altamimi, Z., Sillard, P., Feissel-Vernier, M., 2004 The ITRF2000. International Earth Rotation and Reference Systems Service (IERS). IERS Technical Note 31. Frankfurt am Main, Germany, Verlag des Bundesamtes für Kartographie und Geodäsie, online version at: http://www.iers.org/iers/publications/tn/tn31.

Calais, E., Nocquet, J.M., Jouanne, F., Tardy, M., 2002. Current strain regime in the Western Alps from continuous global positioning system measurements, 1996–2001. Geology 30, 651–654.

D'Agostino, N., Avallone, A., Cheloni, D., D'Anastasio, E., Mantenuto, S., Selvaggi, G., 2008. Active tectonics of the Adriatic region from GPS and earthquake slip vectors. J. Geophys. Res. 113, B12413. doi:10.1029/2008JB005860.

DeMets, C., Gordon, R., Argus, D., Stein, S., 1990. Current plate motions. Geophys. J. Int. 101, 425–478.

DeMets, C., Gordon, R., Argus, D., Stein, S., 1994. Effect of recent revisions to the geomagnetic time scale on estimates of current plate motion. Geophys. Res. Lett. 21, 2191–2194.

Devoti, R., Riguzzi, F., Cuffaro, M., Doglioni, C., 2008. New GPS constraints on the kinematics of the Apennines subduction. Earth and Planetary Sci. Lett. 273, 163–174.

Dewey, J., Pitman, W., Ryan, W., Bonnin, J., 1973. Plate tectonics and the evolution of the Alpine system. Geol. Soc. Am. Bull. 84, 3137–3180.

Dixon, T.H., Mao, A., Bursik, M., Heflin, M., Langbein, J., Stein, R., Webb, F., 1997. Continuous monitoring of surface deformation at Long Valley caldera with GPS. J. Geophys. Res. 102, 12,017–12,034.

Dixon, T.H., Miller, M., Farina, F., Wang, H., Johnson, D., 2000. Present-day motion of the Sierra Nevada block and some tectonic implications for the Basin and Range province, North American Cordillera. Tectonics 19, 1–24.

Favali, P., Funiciello, R., Mattietti, G., Mele, G., Salvini, F., 1993. An active margin across the Adriatic Sea (central Mediterranean Sea). Tectonophysics 219, 109–117.

Fodor, L., Jelen, B., Márton, E., Skaberne, D., Čar, J., Vrabec, M., 1998. Miocene-Pliocene tectonic evolution of the Slovenian Periadriatic fault: implications for Alpine-Carpathian extrusion models. Tectonics 17, 690–709.

Grenerczy, G., Sella, G., Stein, S., Kenyeres, A., 2005. Tectonic implications of the GPS velocity field in the northern Adriatic region. Geophys. Res. Lett. 32, L16311. doi:10.1029/2005GL022947.

Hippolyte, J.-C., Angelier, J., Roure, F., 1994. A major geodynamic change revealed by Quaternary stress patterns in the Southern Apennines (Italy). Tectonophysics 230, 199–210.

Italiano, F., Martelli, M., Martelli, G., Nuccio, P.M., 2000. Geochemical evidence of melt intrusions along lithospheric faults of the Southern Apennines, Italy: geodynamic and seismogenic implications. J. Geophys. Res. 105, 13,569–13,578.

Mao, A., 1998. Geophysical applications of the Global Positioning System [Ph.D. thesis]: Miami, Florida, University of Miami, 149 p.

Mao, A., Harrison, C.G.A., Dixon, T.H., 1999. Noise in GPS coordinate time series. J. Geophys. Res. 104, 2797–2816.

Malinverno, A., Ryan, W., 1986. Extension in the Tyrrhenian Sea and shortening in the Apennines as result of arc migration driven by sinking of the lithosphere. Tectonics 5, 227–245.

McKenzie, D.P., 1972. Active tectonics of the Mediterranean region. Geophys. J. R. Astron. Soc. 30, 109–185.

Oldow, J., Ferranti, L., Lewis, D., Campbell, J., D'Argenio, B., Catalano, R., Pappone, G., Carmignani, L., Conyi, P., Aiken, C., 2002. Active fragmentation of Adria, the north African promontory, central Mediterranean orogen. Geology 30, 779–782.

Platt, J., Behrmann, J., Cunningham, P., Dewey, J., Helman, M., Parish, M., Shepley, M., Wallis, S., Weston, P., 1989. Kinematics of the Alpine arc and motion history of Adria. Nature 337, 158–161.

Pondrelli, S., Salimbeni, S., Ekstrm, G., Morelli, A., Gasperini, P., Vannucci, G., 2006. The Italian CMT data set from 1997 to the present. Phys. Earth Planet. Inter. 159, 286–303. doi:10.1016/j.pepi.2006.07.008.

Sella, G., Dixon, T., Mao, A., 2002. REVEL: a model for recent plate velocities from space geodesy. J. Geophys. Res. 107 (B4), 2081. doi:10.1029/2000JB000033.

Selvaggi, G., Amato, A., 1992. Subcrustal earthquakes in the northern Apennines (Italy): evidence for a still active subduction? Geophys. Res. Lett. 19, 2127–2130.

Serpelloni, E., Anzidei, M., Baldi, P., Casula, G., Galvani, A., 2005. Crustal velocity and strain-rate fields in Italy and surrounding regions: new results from the analysis of permanent and non-permanent GPS networks. Geophys. J. Int. 161, 861–880.

Stein, S., Sella, G., 2006. Pleistocene change from convergence to extension in the Apennines as a consequence of Adria microplate motion. In: Pinter, N., et al. (Ed.), The Adria Microplate: GPS Geodesy, Tectonics and Hazards. Springer, pp. 21–34.

Ward, S., 1990. Pacific–North America plate motions: new results from very long baseline interferometry. J. Geophys. Res. 95, 21965–21981.

Ward, S., 1994. Constraints on the seismotectonics of the central Mediterranean from Very Long Baseline Interferometry. Geophys. J. Int. 117, 441–452.

Weber, J., Vrabec, M., Stopar, B., Pavlovic-Preseren, P., Dixon, T., 2006. The PIVO-2003 experiment: a GPS study of Istria Peninsula and Adria microplate motion, and active tectonics in Slovenia. In: Pinter, N., et al. (Ed.), The Adria Microplate: GPS Geodesy, Tectonics and Hazards. Springer, pp. 305–320.

Westaway, R., 1992. Seismic moment summation for historical earthquakes in Italy: tectonic implications. J. Geophys. Res. 97, 437–464.

Wortel, M., Spakman, W., 2000. Subduction and slab detachment in the Mediterranean–Carpathian region. Science 290, 1910–1917.

Zumberge, J., Heflin, M., Jefferson, D., Watkins, M., Webb, F., 1997. Precise point positioning for efficient and robust analysis of GPS data from large networks. J. Geophys. Res. 102, 5005–5017.